Photosensitized Degradation of DMSO Initiated by PAHs at the Air-Water Interface, as an Alternative Source of Organic Sulfur Compounds to the Atmosphere

Photosensitized degradation of DMSO initiated by PAHs at the air-water interface, as an alternative source of organic sulfur compounds to the atmosphere

Haoyu Jiang[1,2,3,4†], Luca Carena[5†], Yingyao He[6], Yiqun Wang[1,4], Wentao Zhou[1,4], Lihua Yang[6], Tiangang Luan[6], Xue Li[7], Davide Vione[5*], Sasho Gligorovski[1,2,3*]

[1]State Key Laboratory of Organic Geochemistry and Guangdong Provincial Key Laboratory of Environmental Protection and Resources Utilization, Guangzhou Institute of Geochemistry, Chinese Academy of Sciences, Guangzhou 510 640, China

[2]Guangdong-Hong Kong-Macao Joint Laboratory for Environmental Pollution and Control, Guangzhou Institute of Geochemistry, Chinese Academy of Science, Guangzhou 510640, China

[3]Chinese Academy of Science, Center for Excellence in Deep Earth Science, Guangzhou, 510640

[4]University of Chinese Academy of Sciences, Beijing, China

[5]Dipartimento di Chimica, Università degli Studi di Torino, Via Pietro Giuria 5, 10125 Torino, Italy

[6]School of Marine Sciences, Sun Yat-sen University, Guangzhou 510006, China

[7]Institute of Mass Spectrometry and Atmospheric Environment, Jinan University, Guangzhou 510632, China

Submitted to *Journal of Geophysical Research - Atmospheres*

*Corresponding authors: gligorovski@gig.ac.cn
davide.vione@unito.it
†Haoyu Jiang and Luca Carena contributed equally to this work.

ABSTRACT

The photochemical reactions of organic compounds at the water surface lead to the formation of gas-phase molecules that may contribute to new particle formation in the atmosphere. Here, we observe formation of organic sulfur (OS) compounds that are known secondary organic aerosol (SOA) precursors, upon irradiation of aqueous solutions containing typical polycyclic aromatic hydrocarbons (PAHs) such as pyrene, fluoranthene, and phenanthrene, as well as dimethylsulfoxide (DMSO). We suggest a tentative reaction mechanism initiated by excited triplet states of PAHs (^{3}PAHs*), which is supported by theoretical calculations of the reaction Gibbs energies. In all cases, we observe rapid formation of methylsulfonylmethane, ethyl methanesulfonate, methanesulfonic acid, methanesulfinic acid, hydroxymethanesulfonic acid, and 2-hydroxyethenesulfonic acid. We perform a photochemical modeling to estimate the formation rates and quantum yields of these SOA precursors in the atmosphere, which may be generated through the suggested photochemical processes at different latitudes. These results suggest that ubiquitous PAHs and DMSO at the sea surface represent an alternative source of OS compounds during daytime, through photochemical processes that should be considered in future models to better represent the SOA formation processes in the atmosphere.

Keywords: PAHs, SOA, water surface, photochemical reactions, SPI-TOF-MS, UV-VIS spectra

INTRODUCTION

As an important interfacial region between the atmosphere and the sea, the sea surface microlayer (SML) is enriched with organic and inorganic compounds compared to bulk water. Although SML has a thickness of only 1 μm to 1 mm at the sea uppermost surface, which persists at wind speeds of up to 10 m s^{-1} [*Wurl et al.*, 2011], it plays a crucial role in the enhanced photodegradation of substances due to the high intensity of Ultraviolet-Visible (UV-VIS) fraction of sunlight that illuminates the SML [*Vasilkov et al.*, 2001]. Pollutants released from anthropogenic activities will influence the photochemical processes at the SML, and thereby change the air-sea interaction, with still a lack of knowledge about the consequences for coastal air pollution and biogeochemical cycle systems.

Polycyclic aromatic hydrocarbons (PAHs), a common group of primary pollutants produced by biomass burning, coal combustion, and petroleum combustion, are enriched at the surface of both seawater and freshwater via atmospheric deposition [*Lammel*, 2015]. Two to five-ring PAHs at the sea surface mainly come from the interfacial diffusive exchange between the upper sea level and lower marine atmosphere [*González-Gaya et al.*, 2019]. Substantial concentrations of PAHs have been detected to accumulate at the SML, with even 200–400 times enhanced concentrations compared to the water bulk [*J Chen et al.*, 2006; *Cincinelli et al.*, 2001; *Hardy et al.*, 1990; *Lohmann et al.*, 2009; *Seidel et al.*, 2017; *Vácha et al.*, 2006]. At the sea surface, the PAHs concentrations vary from 5 to ~1900 ng L^{-1} [*González-Gaya et al.*, 2019; *Ma et al.*, 2013; *Otto et al.*, 2015; *Pérez-Carrera et al.*, 2007; *Valavanidis et al.*, 2008]. Phenanthrene (PHE), fluoranthene (FLA) and pyrene (PYR) are the most commonly detected PAHs in the coastal SML [*Guitart et al.*, 2007; *Stortini et al.*, 2009], and they even accounted for 92-96% of the total amount of PAHs in a lagoon in Nigeria [*Benson et al.*, 2014].

Dimethylsulfoxide (DMSO) is an ubiquitous organic sulfur (OS) compound in the ocean, and it is one of the main compounds of the marine sulfur cycle [*P A Lee et al.*, 1999]. The main sources of DMSO in the ocean are degradation of phytoplankton [*Andreae*, 1980], photo-induced oxidation of dimethyl sulfide (DMS) [*Barnes et al.*, 2006; *Brimblecombe and Shooter*, 1986], microbial oxidation of DMS [*L Zhang et al.*, 1991], and deposition from the atmosphere due to the high Henry's Law coefficient ($\approx 10^7$ M atm^{-1}) and mass accommodation coefficient (0.10) of DMSO [*Davidovits et al.*, 2006; *González-Gaya et al.*, 2016; *Legrand et al.*, 2001]. The surface tension measurements of aqueous DMSO solutions have indicated that the number densities of this compound at the air-water interface are higher than the concentrations in the water bulk, suggesting surface partitioning effects [*Allen et al.*, 1999].

In the aqueous phase of marine aerosol deliquescent particles, 78% of DMS is oxidized by ozone (O_3) to DMSO [*Hoffmann et al.*, 2016]. Moreover, DMSO exhibits concentrations in the range of 1.5 to 532 nmol L^{-1} from the open ocean to the coastal zones [*Andreae*, 1980; *Asher et al.*, 2017; *Hatton et al.*, 1996; *P Lee and De Mora*, 1996]. Although it mostly occurs in the ocean, DMSO has also been detected in rivers (<2.5–210 nmol L^{-1}) [*Andreae*, 1980], lakes (up to 180 nmol L^{-1}) [*Richards et al.*, 1994], rainwater (2-4 nmol L^{-1}) [*Ridgeway et al.*, 1992], and in aerosols (69–125 pmol m^{-3}) [*Harvey and Lang*, 1986].

One of the main degradation pathways of DMSO is considered to be the microbial consumption or reduction to DMS [*P A Lee et al.*, 1999], as well as the reaction with hydroxyl radicals (OH) [*Barnes et al.*, 2006]. The latter reaction yields methanesulfinic acid (CH_3SO_2H), which in turn may react again with OH radicals to form methanesulfonic acid (CH_3SO_3H) [*Librando et al.*, 2004]. Considering the presence of OH radicals in lakes and sea-surface water, and the occurrence of DMSO at concentrations that are 1-2 orders of magnitude higher than those of DMS, the photochemical oxidation of DMSO may be a relatively more important process than the photo-oxidation of DMS [*P A Lee et al.*, 1999].

Detailed studies, focused on the photochemical processes that occur at the water surface are necessary to improve our understanding of the interactions between the air - water interface and the atmosphere [*Alvarez et al.*, 2012]. The heterogeneous oxidation of PAHs of atmospheric relevance has been investigated in past years [*Donaldson et al.*, 2009; *Monge et al.*, 2010; *Styler et al.*, 2011; *Zhou et al.*, 2019]. However, the structure of gas-phase compounds formed during photodegradation and the reaction pathways leading to their formation are still unclear. Recently, it has been shown that the excited triplet state of fluorene (FLU) can initiate the degradation of DMSO at the air-water interface and produce OS compounds in the atmosphere [*Mekic et al.*, 2020a; *Mekic et al.*, 2020b].

In this study, for the first time to our best knowledge, we found that the detected OS compounds formed by the photochemical degradation of DMSO initiated by sunlight-excited PAHs molecules (PHE, FLA, and PYR) are known precursors of secondary organic aerosols (SOA) in the atmosphere. The gas-phase products formed by light-induced degradation of PAHs/DMSO were assessed by membrane inlet single photon ionization time of flight mass spectrometry (MI-SPI-TOFMS) [*Mekic et al.*, 2020a; *M Zhang et al.*, 2019]. We suggest a tentative reaction pathway of the formed OS compounds during photosensitized degradation of DMSO initiated by excited triplets of PAHs, which is supported by theoretical calculations of the reaction Gibbs energies. Based on the observed experimental data of the formed secondary gas-phase compounds and the relevant formation quantum yields, the formation rates of the OS compounds were estimated with a photochemical model at a global scale.

EXPERIMENTAL

Photoreactor

A double-wall rectangular (5 × 5 × 2 cm) photoreactor made up of borosilicate glass was designed to simulate calm water covered by an organic film made up of DMSO and PAHs.

The photoreactor was thermostated (T = 293 K) by thermostatic bath (LAUDA ECO RE 630 GECO, Germany). Details of the reactor were provided in our previous papers [*Mekic et al.*, 2020a; *Mekic et al.*, 2020b], hence, only brief description is here given. An air flow of 150 mL min^{-1} (0-500 mL min^{-1} HORIBA METRON mass flow controller; accuracy, ±1%) was drifting through the photoreactor during irradiation, to carry the gas-phase product compounds through a 0.5-m long Teflon tube (4 mm I.D.), into the MI-SPI-TOFMS. At the exit of the reactor an air flow of 750 mL min^{-1} (0-1 L min^{-1} HORIBA METRON mass flow controller; accuracy, ±1%) was added to obtain the required 0.9 L min^{-1} flow for MI-SPI-TOFMS.

The three compounds considered in this study, PHE, FLA, and PYR (Sigma-Aldrich, China) with concentrations of 1×10^{-4} mol L^{-1} were dissolved separately in mixtures of DMSO and ultrapure water (10:90 v/v), corresponding to a DMSO concentration of 1.4 mol L^{-1} [*Mekic et al.*, 2020b]. Such high concentrations of the organic co-solvent have been used previously to evaluate the influence of the solvent on PAHs photolysis [*Donaldson et al.*, 2009; *Grossman et al.*, 2016; *Librando et al.*, 2014]. The reactor was filled with 10 mL of freshly prepared solution. A Xenon lamp (Xe, 500 W) was used to irradiate the solutions containing PAHs and DMSO. The spectral irradiance of the Xe lamp was measured with a calibrated spectroradiometer (Ocean Optics, USA) equipped with a linear-array CCD detector, and compared to the sunlight radiation [*Mekic et al.*, 2020a; *Mekic et al.*, 2020b]. There were three experimental conditions including 1 hour-dark, 2h-light irradiation, and 1 hour-dark followed by another 2h-light irradiation of PAHs/DMSO. All experiments were performed in duplicate.

Membrane inlet single photon ionization time of flight mass spectrometry (MI-SPI-TOFMS)

A MI-SPI-ToFMS instrument (SPIMS 3000, Guangzhou Hexin Instrument Co., Ltd., China) was used to detect the gas-phase compounds formed during the photodegradation of DMSO, initiated by irradiated PAHs. A polydimethylsiloxane (PDMS, thickness 0.002 int, Technical Products Inc, USA) membrane was used in the injector of the TOF-MS [*M Zhang et al.*, 2019]. The ionization of the compounds was performed by vacuum ultraviolet (VUV) light emitted by a deuterium (D_2) lamp (Hamamatsu, Japan). Single photon ionization (SPI), with energy of 10.8 eV was used as a "soft" ionization method to detect the gas-phase compounds.

The sampled VOCs are exposed to VUV radiation in the single photon ionization (SPI) source, where they get efficiently ionized if their ionization energy (IE) is lower than the VUV photon energy. Due to the low transfer of excess energy, SPI is a soft ionization technique that is characterized by high molecular ion yield and low degree of fragmentation [*Hanley and Zimmermann*, 2009; *Hua et al.*, 2011; *Wurl et al.*, 2011]. The mass of the product ion equals the analyte mass, greatly facilitating the interpretation of the mass spectrum of complex VOCs samples.

The ToF mass analyzer consists of a double pulsed acceleration region, a field-free drift tube, a reflector and an ion detector. The length of the double pulsed acceleration region is 52 mm. The field-free drift region is 300 mm long and held at an electric field potential of 2200 V, where the ions drift at a constant speed. The reflector is separated into two stages with different field strengths by a grid at earth electric potential. The first and second stages are 90 mm and 35 mm long, respectively. Two micro channel plates (MCP) assembled with chevron-type are used as ion detector. A 350 MHz Analog to Digital Converter (ADC) is used for measuring and recording the output current signal from MCP. The limit of detection (LOD) of

TOF-MS is around 1 ppb for most trace gases. The time resolution of SPI-MS was here set to 5 s.

The raw data were processed with commercial software (SPI-MS 3000 V1.0.1.2.0, Guangzhou Hexin Instrument Co., Ltd., China), where the selected Gauss peaks above a preset threshold are smoothed with a given average number.

Theoretical Calculations

The used structures of all the tentatively identified gaseous compounds are based on the reasonable inferred elemental compositions for a single mass, based on assumptions made by using NIST Chemistry WebBook (https://webbook.nist.gov/chemistry/mw-ser/) and the database of MI-SPI-TOFMS. The possibilities should be considered for the existence of isomers and of different molecular formulas with the same molecular weight. Theoretical calculations were performed to gain some insights into the transformation pathways of ^{3}PHE*, ^{3}PYR*, ^{3}FLA*, and DMSO in the gas phase.

All calculations presented in this work were performed with Gaussian 16W package [*Frisch et al.*, 2016]. The level of B3LYP/6-311G(d,p) was applied for geometry optimizations and frequency calculations for all molecules involved and proposed in the reaction scheme [*Binning Jr and Curtiss*, 1990; *McLean and Chandler*, 1980]. There were no imaginary frequencies for all molecules optimized. Single-point energy calculations were performed at a more expensive level, the M06-2X/Def2-TZVP level [*Weigend*, 2006; *Weigend and Ahlrichs*, 2005; *Y Zhao and Truhlar*, 2008]. The existence of possible geometric isomers and conformers for each species was considered and investigated, and those with lowest calculated Gibbs free energies were selected. Molecular oxygen (O_2), carbon dioxide (CO_2) and water molecules (H_2O) were placed as reactants or products (if needed) to balance atoms in the schemes. Detailed Gibbs free energies for all molecules are presented in Table S1 and S2, and the corresponding Gibbs reaction energies are shown in Scheme 1.

Calculation of the formation quantum yields of gas-phase compounds

Considering that the absorbance of FLA/DMSO, PYR/DMSO and PHE/DMSO ($\varepsilon_{PAH}(\lambda)bC_o$) in the photoreaction system is relatively low, the formation rate R_F of a reaction product upon irradiation of FLA/DMSO, PYR/DMSO and PHE/DMSO can be expressed as follows, allowing for a direct correlation between k_F and Φ_F:

$$R_F = k_F C_o = 2.3 b C_o \Phi_F \int_\lambda p°(\lambda)\varepsilon_{PAH}(\lambda)\, d\lambda \qquad \text{(Eq-1)}$$

where k_F is the first-order formation rate constant of the reaction product, C_o the initial concentration of FLA/DMSO, PYR/DMSO or PHE/DMSO, Φ_F the quantum yield of product formation, $p°(\lambda)$ the incident spectral photon flux density of the lamp, $\varepsilon_{PAH}(\lambda)$ the molar absorption coefficient of the studied PAH (FLA, PYR or PHE) at the wavelength λ (note that DMSO does not absorb lamp radiation significantly, thus the three PAHs are the only light absorbers in the studied systems), and b the optical path length in the photoreactor (1 cm):

It is thus possible to calculate Φ_F from the experimental values of k_F:

$$\Phi_F = \frac{k_F}{2.3 b \int_\lambda p°(\lambda)\varepsilon_{PAH}(\lambda)\, d\lambda} \qquad \text{(Eq-2)}$$

Modeling of the photogeneration of gas-phase compounds in irradiated surface waters on a global scale

The formation quantum yields of the detected gas-phase products were used, together with PAHs (FLA, PYR, PHE) absorption spectra and incident sunlight spectra at the water surface (293-450 nm), as input data for the APEX software (Aqueous Photochemistry of Environmentally-occurring Xenobiotics). The sunlight spectra were referred to different latitudes (0-90°) at the spring equinox (Quick TUV calculator, http://cprm.acom.ucar.edu/Models/TUV/Interactive_TUV). Considering that in this day the

daylight duration is 12 hours in all the globe, each spectrum was referred to 9 am that is located half-way between sunrise (6 am) and midday, thereby constituting a reasonably daily average. By so doing, APEX can compute products formation rate constants (s^{-1}) as a function of latitude and of varying water-chemistry parameters. Water depth was taken as 1 mm, which is representative of the sea-surface microlayer.

RESULTS AND DISCUSSION

Organic sulfur compounds detected by MI-SPI-TOFMS

To detect the gas-phase compounds formed by degradation of PAHs/DMSO in the dark and under irradiation, we applied MI-SPI-TOFMS as a novel promising technology for the on-line and continuous monitoring of VOCs [*Mekic et al.*, 2020a; *M Zhang et al.*, 2019].

Figure 1 shows the Venn diagrams of the observed secondary gas-phase products of the degradation of PAHs/DMSO under light irradiation. It reveals that most of the gas-phase compounds were formed by degradation of PHE/DMSO, and that many of them were the same as the degradation products generated by PYR/DMSO and FLA/DMSO. The Venn diagrams showing the comparison of the formed products under different conditions are presented in Figure S1.

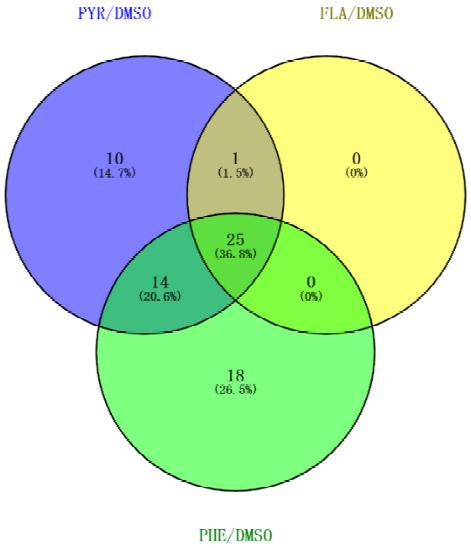

Figure 1: Venn Diagram of the detected molecular formulas for the photodegradation of PAHs/DMSO.

Among all detected compounds, we tentatively identified many unsaturated multifunctional molecules, and OS compounds that are summarized in Table S3 and S4.

Within the studied systems, PHE/DMSO and PYR/DMSO were major contributors to the individually formed gas-phase compounds (Figure 1). Among all detected gas-phase products we highlight the formation of OS compounds, which enable comparison with the corresponding OS compounds identified in ambient aerosol particles (see below).

Comparison of the Identified OS Compounds with Data from Field Measurements

Table 1 shows the comparison of the identified OS compounds under irradiation, with those detected during different field campaigns. It has to be noted that the agreement between the chemical formulas detected in this study and those from field measurements does not necessarily imply the same molecular structure, because multiple structural isomers are possible for each formula [*Mekic et al.*, 2020a; *Nizkorodov et al.*, 2011]. There are 1 and 11 unique tentative OS compounds that emerged upon light irradiation of PYR/DMSO and PHE/DMSO, respectively. There are also 6 shared OS formulas that are released upon light irradiation of both, PYR/DMSO and PHE/DMSO, and 8 shared OS formulas that are generated by all PAHs/DMSO i.e. PYR/DMSO, PHE/DMSO, and FLA/DMSO, in presence of light irradiation.

Table 1: Tentative organic sulfur formulas detected in the present study that were identified in ambient atmospheric aerosols

Reaction system	**m/z**	**Tentative chemical formulas**	**References***
PYR/DMSO	202	$C_7H_6O_5S$	[*Kuang et al.*, 2016]
		$C_8H_{10}O_4S$	[*Wang et al.*, 2016]
PHE/DMSO	168	$C_5H_{12}O_4S$	[*Kuang et al.*, 2016]
	170	$C_3H_6O_6S$	[*Kuang et al.*, 2016]
		$C_4H_{10}O_5S$	[*Kuang et al.*, 2016]
	182	$C_4H_6O_6S$	[*Kuang et al.*, 2016]
		$C_5H_{10}O_5S$	[*Kuang et al.*, 2016; *Shikang Tao et al.*, 2014b; *Wang et al.*, 2016; *Zhu et al.*, 2019]

		$C_6H_{14}O_4S$	[*Kuang et al.*, 2016; *Wang et al.*, 2016]
	192	$C_6H_8O_5S$	[*Wang et al.*, 2016]
	194	$C_6H_{10}O_5S$	[*Kuang et al.*, 2016]
		$C_7H_{14}O_4S$	[*Kuang et al.*, 2016; *Wang et al.*, 2016]
	196	$C_5H_8O_6S$	[*Kuang et al.*, 2016; *Shikang Tao et al.*, 2014b; *Wang et al.*, 2016]
		$C_6H_{12}O_5S$	[*Kuang et al.*, 2016; *Shikang Tao et al.*, 2014b; *Wang et al.*, 2016]
		$C_7H_{16}O_4S$	[*Kuang et al.*, 2016; *Wang et al.*, 2016]
	198	$C_5H_{10}O_6S$	[*Kuang et al.*, 2016; *Shikang Tao et al.*, 2014b; *Wang et al.*, 2016; *Zhu et al.*, 2019]
		$C_6H_{14}O_5S$	[*Kuang et al.*, 2016; *Wang et al.*, 2016]
	204	$C_7H_8O_5S$	[*Wang et al.*, 2016]
	206	$C_7H_{10}O_5S$	[*Kuang et al.*, 2016; *Wang et al.*, 2016]
		$C_8H_{14}O_4S$	[*Kuang et al.*, 2016]
	208	$C_6H_8O_6S$	[*Kuang et al.*, 2016; *Wang et al.*, 2016]
		$C_7H_{12}O_5S$	[*Kuang et al.*, 2016]
		$C_8H_{16}O_4S$	[*Kuang et al.*, 2016; *Shikang Tao et al.*, 2014b; *Wang et al.*, 2016; *Zhu et al.*, 2019]
	210	$C_6H_{10}O_6S$	[*Kuang et al.*, 2016; *Wang et al.*, 2016]
		$C_7H_{14}O_5S$	[*Kuang et al.*, 2016; *Wang et al.*, 2016]
		$C_8H_{18}O_4S$	[*Kuang et al.*, 2016; *Wang et al.*, 2016]
PYR/DMSO, PHE/DMSO	**112**	**CH_4O_4S**(MSAOH)**	
	124	**$C_3H_8O_3S$**(EMS)**	
		$C_2H_4O_4S$	[*Kuang et al.*, 2016]
	152	$C_4H_8O_4S$	[*Kuang et al.*, 2016]
	156	$C_2H_4O_6S$	[*Kuang et al.*, 2016]
	180	$C_5H_8O_5S$	[*Kuang et al.*, 2016]
		$C_6H_{12}O_4S$	[*Kuang et al.*, 2016; *Wang et al.*, 2016]
PAHs/DMSO	**80**	**CH_4O_2S** (MSIA)**	
	94	**$C_2H_6O_2S$**(MSM)**	
	96	**CH_4O_3S**(MSA)**	

126	**$C_2H_6O_4S$**(ESAOH)**	
140	$C_3H_8O_4S$	[*Kuang et al.*, 2016]
154	$C_4H_{10}O_4S$	[*Kuang et al.*, 2016]
	$C_3H_6O_5S$	[*Kuang et al.*, 2016]
166	$C_4H_6O_5S$	[*Kuang et al.*, 2016]
	$C_5H_{10}O_4S$	[*Kuang et al.*, 2016; *Wang et al.*, 2016]
178	$C_5H_6O_5S$	[*Wang et al.*, 2016]

*References related to the chemical formulas of organic sulfur compounds identified in ambient aerosols.
** Bold chemical formulas correspond to the organic sulfur compounds, the formation rates of which were modeled (see section "Photochemical modeling")

In our previous study [*Mekic et al.*, 2020a; *Mekic et al.*, 2020b], we have identified the OS compounds formed during the photodegradation of a mixture of FLU and DMSO. Here we confirm that, in addition to FLU, also the photodegradation of other lightweight PAHs (PYR, FLA, and PHE) mixed with DMSO represents a source of OS compounds that have been detected in field measurements. Among the detected OS formulas, six of them (highlighted in bold font in Table 1) have additionally been identified as SOA precursors [*H Berresheim and Eisele*, 1998; *Ho Berresheim et al.*, 1993; *Dawson et al.*, 2012; *Gaston et al.*, 2010; *Hopkins et al.*, 2008; *Karl et al.*, 2007; *Ning et al.*, 2020]. For this reason, in this work we modeled their formation rates under environmentally relevant conditions (see section "Photochemical Modeling"). These OS compounds can form surfactant films on the aerosol particles in the marine boundary layer, by which means they influence the surface tension and hygroscopicity of the particles [*Decesari et al.*, 2011; *S. Tao et al.*, 2014a].

Time Evolution of OS Compounds

The photochemical degradation of PAHs/DMSO releases a number of OS compounds in the gas phase. We observed rapid formation of methylsulfonylmethane ($(CH_3)_2SO_2$, MSM), ethyl methanesulfonate ($CH_3SO_3C_2H_5$, EMS), methanesulfonic acid (CH_3SO_3H, MSA),

methanesulfinic acid (CH_3SO_2H, MSIA), hydroxymethanesulfonic acid (CH_4O_4S, MSAOH), and 2-hydroxyethenesulfonic acid ($C_2H_5O_4SH$, ESAOH). All these compounds have been found in particles in coastal as well as inland regions, and identified as SOA precursors [*H Berresheim and Eisele*, 1998; *Ho Berresheim et al.*, 1993; *Dawson et al.*, 2012; *Gaston et al.*, 2010; *Hopkins et al.*, 2008; *Karl et al.*, 2007; *Ning et al.*, 2020]. Although, in the past years, the formation chemistry of sulfuric acid in the marine atmosphere has been extensively studied, the same did not happen for other sulfur-containing organic compounds such as MSIA, MSA, MSM, EMS, and ESAOH. The gas-phase MSA and MSIA are peculiarly important species for the initial stage of new particle formation (NPF) [*H Chen et al.*, 2016; *Schobesberger et al.*, 2013; *H Zhao et al.*, 2017]. The discrepancy between modeled and measured vertical profiles of MSA suggested a missing source close to the ocean surface, which is much stronger than the estimated chemical production from DMS oxidation [*S H Zhang et al.*, 2014]. The comparison between daytime and before-dawn measurements indicated that this strong source of MSA is photolytically enhanced in daytime; it has been suggested that gaseous DMSO could be the potential precursor of MSA [*S H Zhang et al.*, 2014]. Here, we show that the photosensitized reactions of DMSO by light-excited PAHs enriched at water surface could represent an important source of gaseous MSA formation near the ocean surface. Figures 2A and 2B show typical time evolution profiles of MSIA and MSA, formed upon irradiation of PAHs/DMSO. The formation profiles of MSM, EMS, MSAOH and ESAOH are shown in Figure S2. MSIA can be formed via OH radical addition to DMSO with the removal of a CH_3 radical, while MSA as the simplest organosulfate is mainly formed though gas-phase SO_2 oxidation of DMS and heterogeneous oxidation of DMSO [*Barnes et al.*, 2006; *Glasow and Crutzen*, 2004]. Here, we present alternative formation pathways of MSIA and MSA through photochemical reactions of PAHs with DMSO.

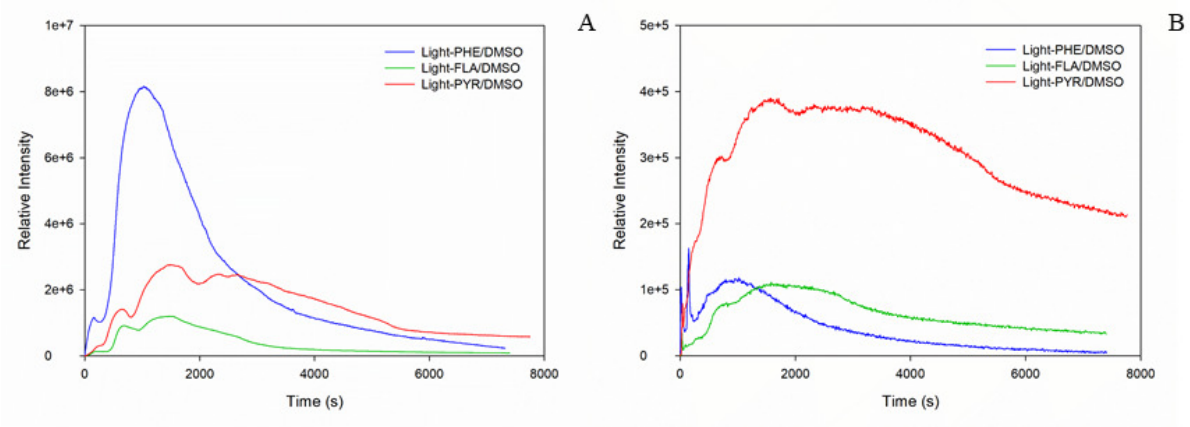

Figure 2: Formation profiles of MSIA (m/z=80) upon photodegradation of PAHs/DMSO (Panel A). Formation profiles of MSA (m/z=96) upon photodegradation of PAHs/DMSO (Panel B).

Figure 2A shows that gas-phase MSIA is promptly formed upon light irradiation of FLA/DMSO, PYR/DMSO, and PHE/DMSO: in about 15 to 20 min, its signal intensity increases in all three cases. In the case of PHE/DMSO the signal intensity of MSIA promptly decreases after the maximum, presumably due to its consumption and the formation of other products. During the photodegradation of FLA/DMSO and PYR/DMSO, the intensity of formed MSIA remains approximately stable during a period of ca.1 hour (most likely because the formation of MSIA balances its consumption), before decreasing in these cases as well. Similar behavior was observed for the formation profiles of MSA upon photodegradation of FLA/DMSO, PYR/DMSO, and PHE/DMSO (Figure 2B).

To support the importance of the suggested photochemistry of PAHs/DMSO, we explored the tentative reaction pathway(s) responsible for the production of OS compounds, and developed a photochemical model to simulate the formation rates of the organic sulfur compounds under environmentally relevant conditions.

Photodegradation pathway of DMSO initiated by excited triplets of FLA, PYR and PHE

In addition to OS compounds, a number of unsaturated multifunctional compounds were also detected. A reaction mechanism of FLA/DMSO, PYR/DMSO, and PHE/DMSO degradation is here suggested, based on the information obtained from the detected tentative products in the gas phase and on quantum chemistry calculations. Because the three PAHs are the only light-absorbing compounds that can act as photosensitizers, the initial step we propose is the photoexcitation of PAHs through a $\pi \rightarrow \pi^*$ electronic transition, followed by intersystem crossing to produce the excited triplet states (^{3}PAHs*) [*Barbas et al.*, 1997; *Barbas et al.*, 1996; *Fasnacht and Blough*, 2003; *Fasnacht et al.*, 2002]. It has been demonstrated that ^{3}PAHs* can react with DMSO in water/DMSO solution [*Mekic et al.*, 2020a], including the pathway leading to the formation of singlet oxygen ($^1O_2$) through energy transfer to triplet-state oxygen ($^3O_2$) [*Wilkinson et al.*, 1995], the pathway yielding hydroxyl (OH) radicals through water oxidation by ^{3}PAHs* [*Brigante et al.*, 2010], and the pathway leading to the formation of radicals through electron transfer. The formation of unsaturated compounds is accompanied with free radicals and reactive oxygen, which favor the generation of OS products.

Scheme 1: *Detailed reaction mechanism describing the formation of gas phase products initiated by ^{3}PAHs* and DMSO. Numbers in brackets, written below each molecule, present compound designations to follow the discussion better with the Scheme 1. All identified products are framed into red or orange rectangles (see Tables S3, S4 for additional details on their detection). The numbers near each reaction arrow represent Gibbs energies arising from quantum chemistry calculations.*

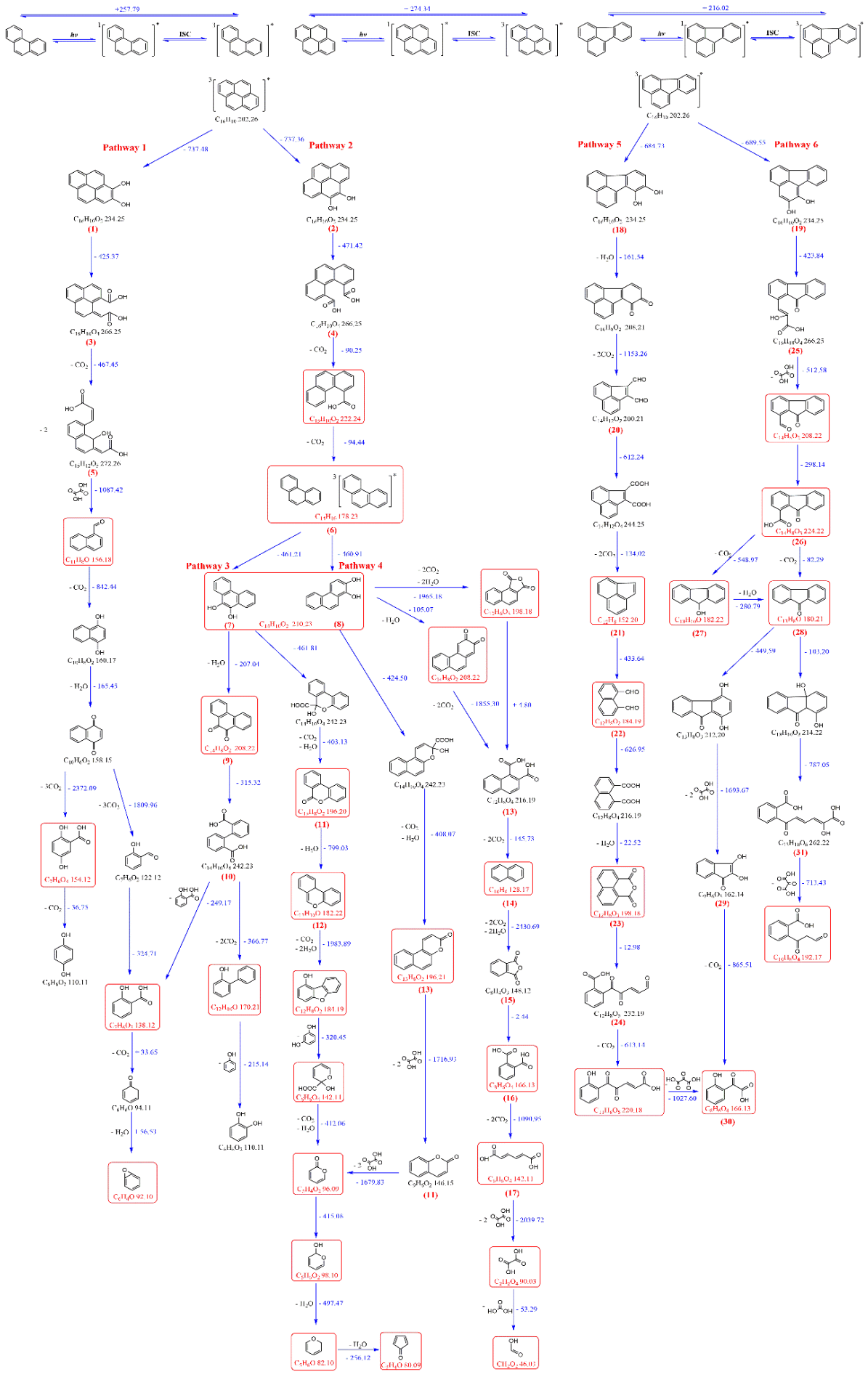
+257.79
hν
ISC
− 274.34
hν
ISC
− 216.02
hν
ISC
C16H10 202.26
Pathway 1
- 737.48
Pathway 2
- 737.36
C16H10O3 234.25
(1)
- 425.37
C18H18O4 266.25
(3)
- CO2
- 467.45
C15H12O2 272.26
(5)
- 2
- 1087.42
C11H8O 156.18
- CO2
- 842.44
C10H8O2 160.17
- H2O
- 165.45
C10H6O2 158.15
- 3CO2
- 2372.09
- 3CO2
- 1809.96
C5H6O4 154.12
- CO2
- 36.75
C4H6O2 110.11
C7H6O2 122.12
- 324.71
C7H6O3 138.12
- CO2
- 33.65
C6H6O 94.11
- H2O
- 56.53
C6H4O 92.10
C16H10O3 234.25
(2)
- 471.42
C18H16O5 266.25
(4)
- CO2
- 90.25
C15H10O2 222.24
- CO2
- 94.44
C13H10 178.23
(6)
- 461.21
- 460.91
Pathway 3
Pathway 4
C13H10O2 210.23
(7)
(8)
- H2O
- 207.04
C14H8O2 208.22
(9)
- 315.32
C16H10O4 242.23
(10)
- 249.17
- 2CO2
- 366.77
C12H10O 170.21
- 215.14
C6H6O2 110.11
- 461.81
C15H10O4 242.23
- CO2
- H2O
- 403.13
C13H10O2 196.20
(11)
- H2O
- 799.03
C13H10O 182.22
(12)
- CO2
- 2H2O
- 1983.89
C12H8O2 181.19
- 320.45
C8H6O5 142.11
- CO2
- H2O
- 412.06
C5H4O2 96.09
- 415.08
C5H6O2 98.10
- H2O
- 497.47
C5H6O 82.10
- H2O
- 256.12
C4H4O 80.09
- 1679.83
C9H6O2 146.15
(11)
- 1716.93
- 424.50
2CO2
- 2H2O
- 1965.18
- 105.07
- H2O
C13H8O3 198.18
C14H8O2 208.22
- 2CO2
- 1855.30
+ 1.80
C14H10O4 242.23
- CO2
- H2O
- 408.07
C12H8O2 196.21
(13)
C12H10O2 216.19
(13)
- 2CO2
- 145.73
C16H8 128.17
(14)
- 2CO2
- 2H2O
- 2130.69
C9H10O2 148.12
(15)
- 2.54
C8H6O5 166.13
(16)
- 2CO2
- 1090.95
C5H6O4 142.11
(17)
- 2
- 2039.72
C2H2O4 90.03
- HO-OH
- 52.29
CH2O2 46.03
Pathway 5
Pathway 6
C16H10O3 234.25
(18)
684.23
689.55
C16H10O3 234.25
(19)
- H2O
- 161.54
C14H8O2 208.21
- 2CO2
- 1153.26
C14H12O2 200.21
(20)
- 612.24
C13H8O3 244.25
- 2CO2
- 134.02
C13H8 152.20
(21)
- 433.64
C12H8O2 184.19
(22)
- 626.95
C12H8O4 216.19
- H2O
- 22.52
C14H8O2 198.18
(23)
- 12.98
C12H8O2 232.19
(24)
- CO2
- 613.14
C13H10O5 220.18
- 1027.60
C16H10O2 234.25
(19)
- 423.84
C15H10O4 266.25
(25)
- 512.58
C14H8O2 208.22
- 298.14
C13H8O3 224.22
(26)
- CO2
- 548.97
- CO2
- 82.29
C13H10O 182.22
(27)
- H2O
- 280.79
C13H8O 180.21
(28)
- 349.59
- 103.20
C12H8O2 212.20
C13H10O2 214.22
- 787.05
C15H10O4 262.22
(31)
- 2
- 1693.67
- 713.43
C6H6O3 162.14
(29)
- CO2
- 865.51
C10H8O4 192.17
C8H6O4 166.13
(30)

In this study, the comprehensive reaction schemes we propose account for the majority of the detected unsaturated multifunctional compounds and the above-mentioned OS compounds emerging from the photosensitized processing of DMSO by light-excited PAHs (^{3}PYR*, ^{3}FLA* and ^{3}PHE*), at the air-water interface. As shown in Scheme 1, the general photodegradation mechanism initiated by ^{3}PAH* could be divided into 6 proposed pathways initiated by ^{3}PYR*, ^{3}FLA* and ^{3}PHE*, which are complementary to the reaction mechanisms suggested by previous studies [*Cao et al.*, 2015; *Liang et al.*, 2006; *Rehmann et al.*, 2001; *van Herwijnen et al.*, 2003]. During the photodegradation of PYR, PHE could also be one of the intermediate products participating to the oxidation reactions. Pathways 1 and 2 describe the reactions of ^{3}PYR* in the presence of O_2 to yield 1,2-Pyrenediol (1) and 4,5-dihydroxy-pyrene (2). The degradation of the latter compounds could involve O_2 attack to the aromatic ring (at positions corresponding to the 1/2 and 4/5 of PYR, see Figure S3), allowing the ring to open and yielding pyrene-dicarboxylic acids (3,4). In Pathway 1, further degradation could be initiated at positions corresponding to 8a/10a of PYR, triggering another phenyl ring opening (5) and generating smaller degradation products with aromatic ring structures. In pathway 2, by the cleavage of carboxyl groups, PHE (6) could be formed after a decarboxylation pathway.

Pathways 3 and 4 describe the degradation of PHE (6), yielding 9,10-dihydroxy-phenanthrene (7) and 1,2-dihydroxy-phenanthrene (8). In pathway 3, the photooxidation of 9,10-phenanthraquinone (9) might yield the biphenyl compound (10) by ring opening at the position that corresponds to the 8a/10a of PHE (Figure S3). The substituted biphenyl is subsequently decomposed into a single aromatic structure after photooxidation. Additionally, O_2 attack might also afford a ring expanded lactone and further transformation into xanthone (11) and xanthene (12). In pathway 4, the photodegradation of 1,2-anthraquinone could yield naphthopyrone (13), which could be subsequently converted into smaller molecules by

cleavage of the aromatic ring. Meanwhile, phenyl ring opening at the positions corresponding to the 4a/10a or 8a/4b of PHE would yield in succession 1,2-naphthalenedicarboxylic acid (13), naphthalene (NAP) (14), phthalic anhydride (15), and phthalic acid (16). Subsequently, with a last phenyl ring opening followed by oxidative transformation, one could account for the generation of an acyclic structure (muconic acid (17)), which might then be degraded into smaller molecules upon photooxidation and decarboxylation.

Pathways 5 and 6 describe the reaction of ^{3}FLA* in the presence of O_2 to yield 9,10-dihydroxy-fluoranthene (18) and 1,2-dihydroxy-fluoranthene (19). In pathway 5, degradation of (18) could involve O_2 attack to the saturated phenyl ring to form $C_{14}H_{12}O_2$ (20) and acenaphthylene (21). Activation of the saturated five-member ring of (21) at the 6b/10a position could give naphthalene-2,3-dicarbaldehyde (22), which could then be converted into 1,8-naphthalic anhydride (23) and the compound $C_{12}H_8O_5$ (24) having a single aromatic ring.

In pathway 6 a ring opening, following O_2 attack to (19) to give (25), would enable further formation of 9-fluorenone-1-carboxylic acid (26), followed by the production of 9-fluorenol (27) and 9-fluorenone (28). Further degradation would occur upon oxidation, at positions corresponding to the 6b/10a and 6a/6b of FLA, with ring cleavage and production of 1,2-dihydroxy-indenone (29), 2-hydroxyphenylglyoxylic acid (30), and $C_{13}H_{10}O_6$ (31).

Moreover, DMSO can be oxidized by O(^{3}P) and OH radical formed during the reaction of DMSO and ^{3}PAH*, yielding further radical species and OS compounds (Scheme 2). The OS compounds formation mechanisms from DMSO + ^{3}PAH* were suggested to be generally divided into 3 possible pathways of free radical production. Pathway 1 describes the reaction between DMSO and OH radical that yields MSIA (1) and methyl radical (CH_3) [*Arsene et al.*, 2002; *Falbe-Hansen et al.*, 2000; *González-García et al.*, 2006; *Urbanski et al.*, 1998]. There could then be an attack of a CH_3 radical to form MSM (2) via oxidation of MSIA [*Arsene et al.*, 2002; *Falbe-Hansen et al.*, 2000].

Scheme 2: *Reaction mechanism describing the formation of gas phase products initiated by O(^{3}P) and OH radical oxidation of DMSO. Numbers in brackets, written below each molecule, present compound designations to follow the discussion better with Scheme 2. The identified OS products as SOA precursors are framed into red rectangles. The numbers near each reaction arrow represent Gibbs energies arising from quantum chemistry calculations.*

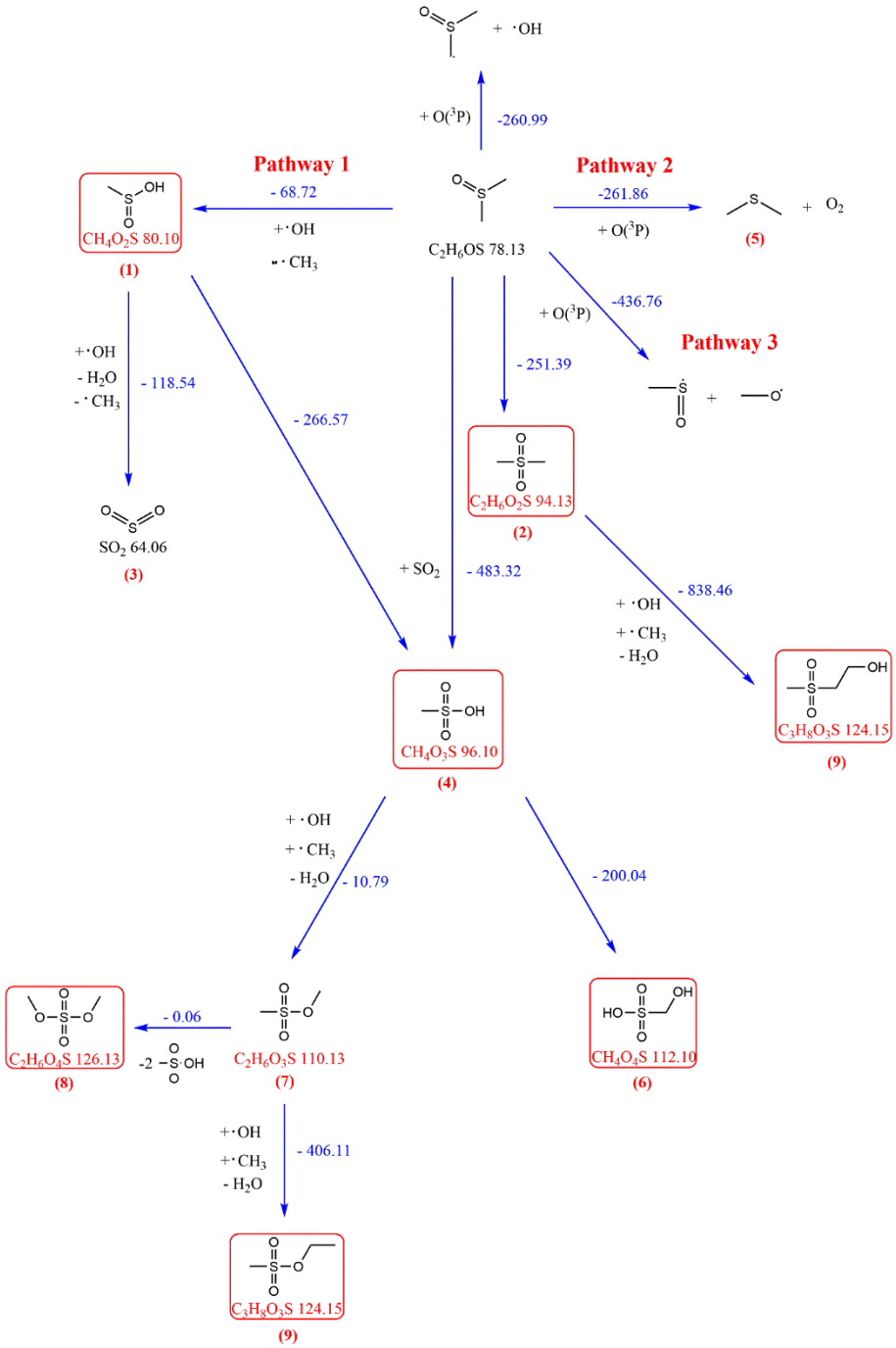

It has been reported that the OH-addition route in the gas-phase atmospheric oxidation of DMSO would result in high yields of SO_2 (3), which is a precursor of H_2SO_4, while MSA (4) would be produced by a liquid-phase reaction [*Allen et al.*, 1999; *Arsene et al.*, 2002; *Kukui et al.*, 2003; *Urbanski et al.*, 1998]. In Pathway 2, the attack of $O(^3P)$ allows transformation of DMSO to DMS (5) and the release of oxygen gas [*Mandal et al.*, 2012; *Pope et al.*, 2002]. In pathway 3, the continuous oxygen attack on DMSO triggers the formation of an alkoxy (RO) radical [*Mandal et al.*, 2012; *Riffault et al.*, 2003]. With the formation of these radicals and oxygen, MSM (2) could be further oxidized into MSAOH (6), $C_2H_6O_3S$ (7), ESAOH (8) and EMS (9) sequentially.

Photochemical model

Initially the model was set to calculate the formation quantum yields of MSIA, MSM, MSA, MSAOH, EMS and ESAOH upon irradiation of FLA/DMSO, PYR/DMSO and PHE/DMSO. Quantum yields were calculated by using the equation $\Phi_F = k_F\, C_0\, [2.3 \int_\lambda p°(\lambda)\, A(\lambda)\, d\lambda]^{-1}$, as described in the experimental section. The values of k_F for each OS compound were computed from the fit of the relevant temporal profiles recorded in the PAH/DMSO experiments, as those of Figure 3, with an *ad-hoc* equation of the type $S = S_p\, [1 - \exp(-k_F\, t)]$. Here, S is the signal, S_p a constant and t the irradiation time. Only that part of the temporal profiles where S increases and reaches a maximum/plateau was considered for the fit, because the decaying part is not predicted by the fit equation. The results of the formation quantum yield calculations are reported in Table 2.

Table 2: Formation quantum yields Φ_F of the main investigated OS compounds (those known to be SOA precursors) upon irradiation of the mixtures FLA/DMSO, PYR/DMSO and PHE/DMSO.

	FLA/DMSO	PYR/DMSO	PHE/DMSO
MSIA	4×10^{-3}	5×10^{-3}	0.13
MSM	5×10^{-3}	3.1×10^{-2}	0.24
MSA	5×10^{-3}	3.1×10^{-2}	0.21
MSAOH	1.5×10^{-2}	2.9×10^{-2}	0.21
EMS	1.0×10^{-2}	2.4×10^{-2}	0.02
ESAOH	2×10^{-3}	2.4×10^{-2}	0.11

The photochemical model provides insight into the possible environmental significance of this process, as well as the formation rates of the six OS compounds as a function of latitude, under environmentally relevant conditions. The first finding suggested by the model is that water chemistry (and especially the dissolved organic carbon, DOC) has very little impact on the photogeneration kinetics of OS compounds (data not shown). Indeed, in a 1 mm thick surface microlayer the competition for sunlight irradiance between PAHs and other light-absorbing species (most notably the chromophoric dissolved organic matter, CDOM) is very limited. Therefore, other light-absorbing organic compounds have few chances to interfere with light absorption by PAHs.

That said, the trends with latitude of the predicted first-order rate constants k_F of OS compound formation are reported in Figure 3 (3a: FLA/DMSO; 3b: PYR/DMSO; 3c: PHE/DMSO). With the relevant input data, the used software carries out numerical integration of the following equation:

$$k_F = 2.3\, d\ \Phi_F \int_{\lambda} p°(\lambda)\, \varepsilon_{PAH}(\lambda)\, d\lambda \qquad \text{(Eq-3)}$$

where d = 1 mm = 10^{-3} m is water depth referred to the SML, Φ_F has the values reported in Table 2, and $p°(\lambda)$ depends on the latitude (TUV calculator).

Figure 3 shows that, under spring-equinox conditions, kinetics are clearly decreasing when going from the equator (0° latitude, 45° solar zenith angle in mid-morning) to the poles (90° latitude, 90° solar zenith angle in mid-morning). It is also suggested by Figure 3 that, coherently with our experimental findings and the data of Table 2, the studied PAHs induce production of the same OS compounds, but with different formation rate constants. In particular, irradiated FLA/DMSO mainly produces MSAOH and EMS, while PYR/DMSO and PHE/DMSO mainly yield MSM, MSA and MSAOH.

Although DOC as well as its light-absorption properties vary over the world's oceans [*Nelson and Siegel*, 2013], here the first-order formation rate constants of OS compounds showed negligible dependence on the DOC, while they seem to be highly dependent on latitude. This is mainly due to the changes in solar irradiance from the equator to the poles.

These findings allowed, for instance, for the assessment of the global distribution of the formation rate constants of SA upon irradiation of FLA/DMSO, PYR/DMSO, and PHE/DMSO (Figure 4). Note that the maps for FLA/DMSO and PYR/DMSO are comparable, in agreement with the comparable formation rate constants of SA shown in Figure 3a/b. In contrast, in the case of PHE/DMSO the predicted SA formation is lower, again in agreement with the data reported in Figure 3. In this case, the relatively high quantum yield of SA formation (see Table 2) is offset by low radiation absorption by PHE.

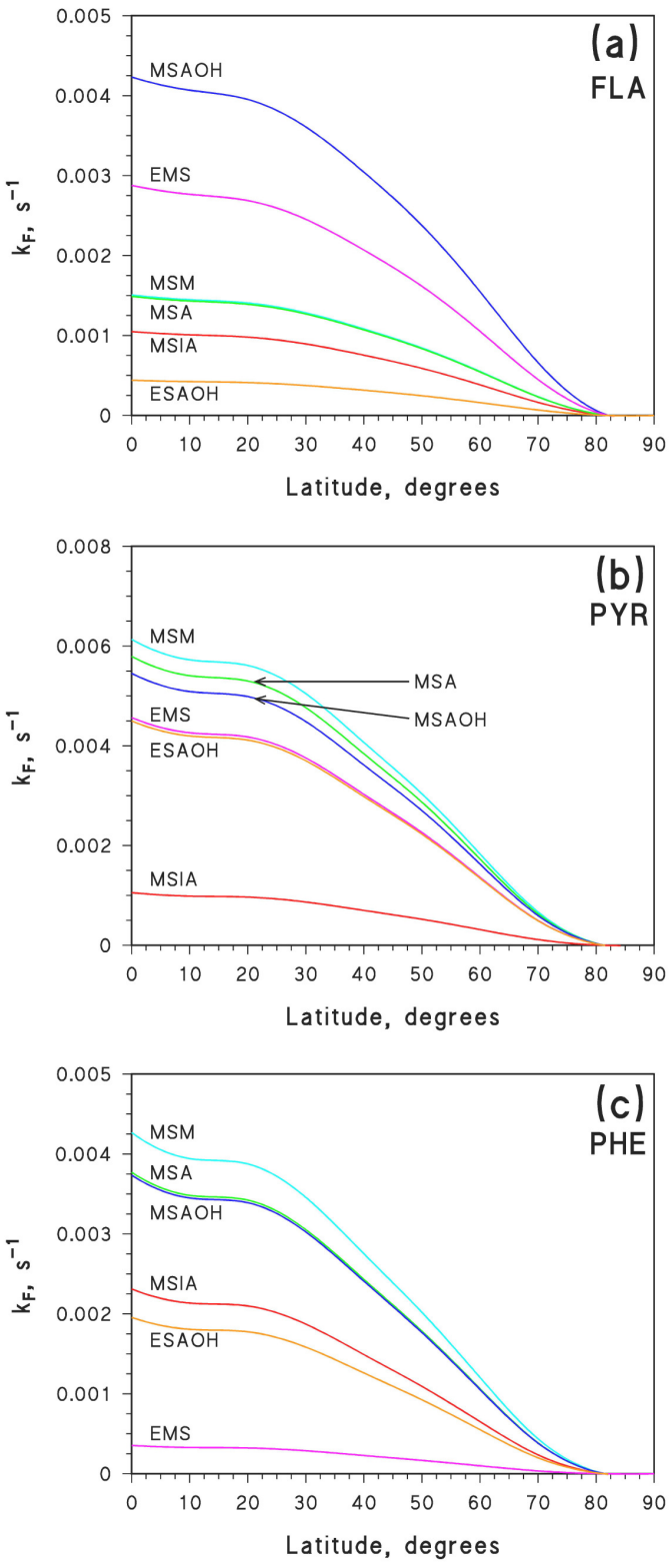

Figure 3: Modeled first-order rate constants of OS compound formation (k_F) from irradiated **(a)** FLA/DMSO; **(b)** PYR/DMSO, and **(c)** PHE/DMSO, as a function of the latitude (0° = equator, 90° = poles). It was assumed DOC = 1 $mg_C\ L^{-1}$, but the DOC has negligible effect on the modeled photoreactions (water depth d = 1 mm). Sunlight conditions refer to the spring equinox in mid-morning, which is a reasonable daytime average.

(a) FLA/DMSO

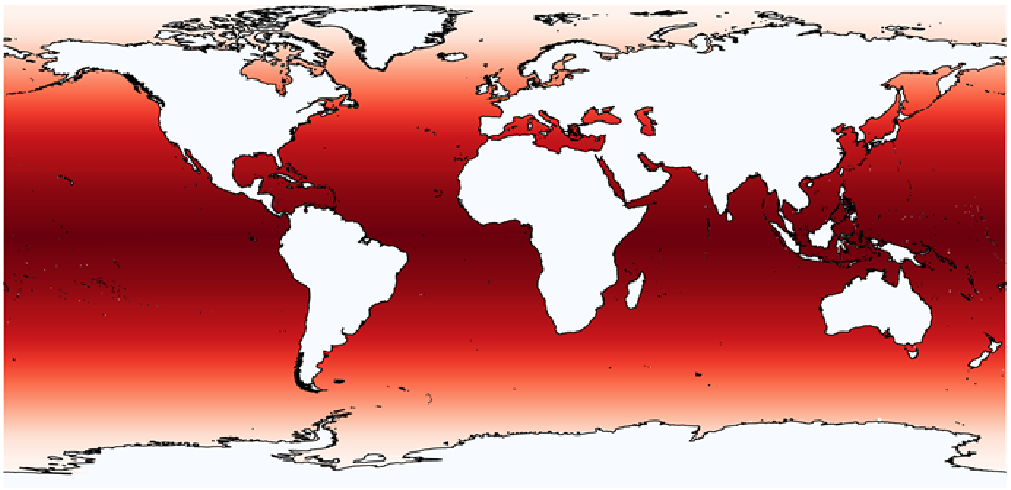

(b) PYR/DMSO

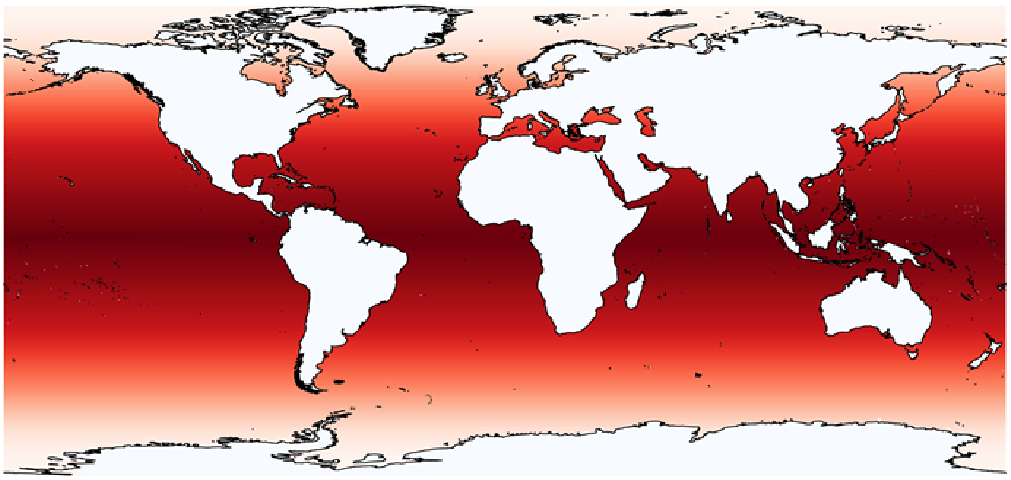

(c) PHE/DMSO

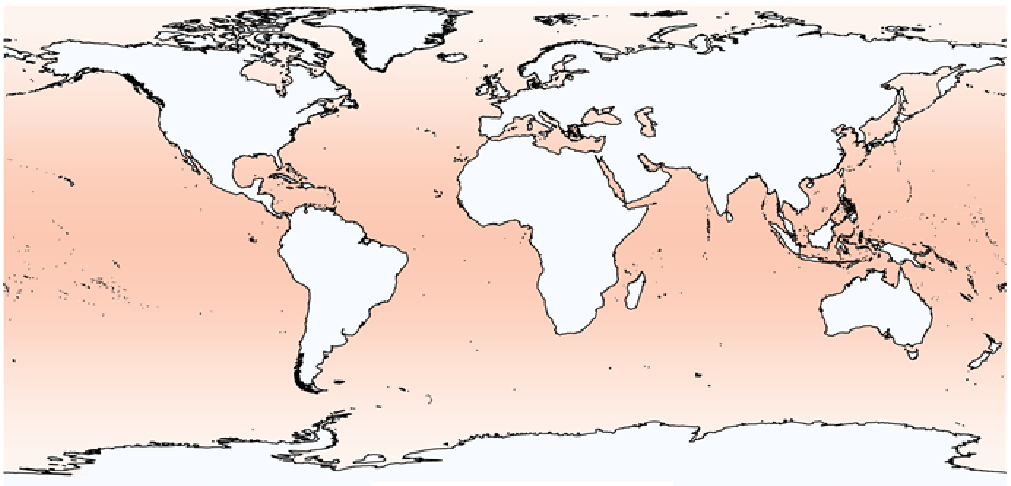

k_{form} (SA), $\cdot 10^{-3}$ s^{-1}

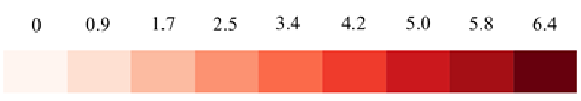

Figure 4: Global distribution of the modeled first-order rate constants of SA formation from irradiated **(a)** FLA/DMSO; **(b)** PYR/DMSO, and **(c)** PHE/DMSO. It was assumed DOC = 1 $mg_C\ L^{-1}$, but the DOC has negligible effect of the modeled photoreactions (water depth d = 1 mm). Sunlight conditions refer to the spring equinox in mid-morning, which is a reasonable daytime average. Maps were made by means of the software QGIS (QGIS, 2020).

Conclusions and Implications

In the present study, it was shown that the photochemistry of PAHs with DMSO at the sea surface may initiate the formation of many gas-phase organic sulfur compounds, some of which are well-known SOA precursors. In all cases the formation of MSM, EMS, MSIA, MSAOH and ESAOH was observed, their formation quantum yields were calculated based on the experimental data of formation rate constants and light absorption by PAHs, and their formation rates were modeled as a function of latitude for a water depth of 1 mm, which is representative of the sea SML. The obtained results may better explain field observations of new particle formation events in the atmosphere above the ocean surface, which are different than the primary emitted aerosol particles from biological processes occurring in the ocean [*O'Dowd et al.*, 2004].

The photosensitized transformation of DMSO by the excited triplet states of PAHs suggested in this study can contribute to the sulfur cycle in the SML, and it could be an important process controlling the volatility and efflux of sulfur from the oceans into the atmosphere [*Mopper*, 2002]. We found that DMSO was oxidized to photochemically stable species including MSIA and MSA, a process that results in the formation of cloud condensation nuclei (CCN), which in turn affect the Earth's radiative balance [*Mopper*, 2002].

Acknowledgements

This study was supported by China Postdoctoral Science Foundation (N°: 2019M653105) and Guangdong Foundation for Program of Science and Technology Research (N°: 2114050002566), funded by Institute Director Foundation of GIG (N°: 2019SZJJ-10). This study was financially supported by the Chinese Academy of Science, International Cooperation Grant (N°: 132744KYSB20190007), National Natural Science Foundation of China (N°: 41773131, and N°: 41977187), State Key Laboratory of Organic Geochemistry, Guangzhou Institute of Geochemistry (SKLOG2020-5, and KTZ_17101).

The authors thank Jiangping Liu, Huifan Deng and Gwendal Loisel for their assistance in the lab analysis. All data in this manuscript are freely available upon request through the corresponding author (gligorovski@gig.ac.cn and davide.vione@unito.it).

Author Contributions

H.J. and L.C. contributed equally to this work. D.V. and S.G. designed the research; H.J., L.C. and S.G. wrote the paper; H.J. and Y.W. performed the gas-phase studies; H.J. interpreted the SPI-TOF-MS data and speculated reaction pathways; W.Z. and X.L. contributed to the SPI-TOF-MS data analysis and relevant discussion. Y.H. carried out the Gibbs energies theoretical calculation of the reaction initiated by ^{3}PAH*; Y.H, L.Y. and T.L. contributed to the relevant discussion of reaction mechanisms; L.C., H.J. and D.V. performed and interpreted the photochemical model. All of the authors contributed to revising the manuscript and approved the final version.

References

Allen, H. C., D. Gragson, and G. Richmond (1999), Molecular structure and adsorption of dimethyl sulfoxide at the surface of aqueous solutions, *J. Phys. Chem. B*, *103*(4), 660-666.

Alvarez, E. G., H. Wortham, R. Strekowski, C. Zetzsch, and S. Gligorovski (2012), Atmospheric Photosensitized Heterogeneous and Multiphase Reactions: From Outdoors to Indoors, *Environ. Sci. Technol.*, *46*(4), 1955-1963.

Andreae, M. O. J. L. (1980), Dimethylsulfoxide in marine and freshwaters, *Limnol. Oceanogr.*, *25*(6), 1054-1063.

Arsene, C., I. Barnes, K. H. Becker, W. F. Schneider, T. T. Wallington, N. Mihalopoulos, and I. V. J. E. s. Patroescu-Klotz (2002), Formation of methane sulfinic acid in the gas-phase OH-radical initiated oxidation of dimethyl sulfoxide, *Environ. Sci. Technol.*, *36*(23), 5155-5163.

Asher, E., J. W. Dacey, D. Ianson, A. Peña, and P. D. Tortell (2017), Concentrations and cycling of DMS, DMSP, and DMSO in coastal and offshore waters of the Subarctic Pacific during summer, 2010‐2011, *J. Geophys. Res. Oceans*, *122*(4), 3269-3286.

Barbas, J. T., M. E. Sigman, R. Arce, and R. Dabestani (1997), Spectroscopy and photochemistry of fluorene at a silica gel/air interface, *J. Photochem. Photobiol. A: Chem.*, *109*(3), 229-236.

Barbas, J. T., M. E. Sigman, R. J. E. s. Dabestani, and technology (1996), Photochemical oxidation of phenanthrene sorbed on silica gel, *Environ. Sci. Technol.*, *30*(5), 1776-1780.

Barnes, I., J. Hjorth, and N. Mihalopoulos (2006), Dimethyl sulfide and dimethyl sulfoxide and their oxidation in the atmosphere, *Chem. Rev.*, *106*(3), 940-975, doi:10.1021/cr020529+.

Benson, N. U., J. P. Essien, F. E. Asuquo, and A. L. Eritobor (2014), Occurrence and distribution of polycyclic aromatic hydrocarbons in surface microlayer and subsurface seawater of Lagos Lagoon, Nigeria, *Environ. Monit. Assess.*, *186*(9), 5519-5529.

Berresheim, H., and F. Eisele (1998), Sulfur chemistry in the Antarctic Troposphere Experiment: An overview of project SCATE, *J. Geophys. Res-Atmos*, *103*(D1), 1619-1627.

Berresheim, H., F. Eisele, D. Tanner, L. McInnes, D. Ramsey‐Bell, and D. Covert (1993), Atmospheric sulfur chemistry and cloud condensation nuclei (CCN) concentrations over the northeastern Pacific coast, *J. Geophys. Res-Atmos*, *98*(D7), 12701-12711.

Binning Jr, R., and L. Curtiss (1990), Compact contracted basis sets for third‐row atoms: Ga–Kr, *J. Comput. Chem.*, *11*(10), 1206-1216.

Brigante, M., T. Charbouillot, D. Vione, and G. Mailhot (2010), Photochemistry of 1-nitronaphthalene: A potential source of singlet oxygen and radical species in atmospheric waters, *J. Phys. Chem. A*, *114*(8), 2830-2836.

Brimblecombe, P., and D. Shooter (1986), Photo-oxidation of dimethylsulphide in aqueous solution, *Mar. Chem.*, *19*(4), 343-353.

Cao, J., Q. Lai, J. Yuan, and Z. Shao (2015), Genomic and metabolic analysis of fluoranthene degradation pathway in Celeribacter indicus P73 T, *Sci. Rep.*, *5*, 7741.

Chen, H., M. E. Varner, R. B. Gerber, and B. J. Finlayson-Pitts (2016), Reactions of Methanesulfonic Acid with Amines and Ammonia as a Source of New Particles in Air, *J. Phys. Chem. B*, *120*(8), 1526-1536, doi:10.1021/acs.jpcb.5b07433.

Chen, J., F. S. Ehrenhauser, K. T. Valsaraj, and M. J. Wornat (2006), Uptake and UV-photooxidation of gas-phase PAHs on the surface of atmospheric water films. 1. Naphthalene, *J. Phys. Chem. A*, *110*(29), 9161-9168.

Cincinelli, A., A. M. Stortini, M. Perugini, L. Checchini, and L. Lepri (2001), Organic pollutants in sea-surface microlayer and aerosol in the coastal environment of Leghorn - (Tyrrhenian Sea), *Mar. Chem.*, *76*(1-2), 77-98, doi:10.1016/s0304-4203(01)00049-4.

Davidovits, P., C. E. Kolb, L. R. Williams, J. T. Jayne, and D. R. Worsnop (2006), Mass accommodation and chemical reactions at gas− liquid interfaces, *Chem. Rev.*, *106*(4), 1323-1354.

Dawson, M. L., M. E. Varner, V. Perraud, M. J. Ezell, R. B. Gerber, and B. J. Finlayson-Pitts (2012), Simplified mechanism for new particle formation from methanesulfonic acid, amines, and water via experiments and ab initio calculations, *Proc. Natl. Acad. Sci. U.S.A.*, *109*(46), 18719-18724.
Decesari, S., E. Finessi, M. Rinaldi, M. Paglione, S. Fuzzi, E. Stephanou, T. Tziaras, A. Spyros, D. Ceburnis, and C. O'Dowd (2011), Primary and secondary marine organic aerosols over the North Atlantic Ocean during the MAP experiment, *J. Geophys. Res-Atmos*, *116*(D22).
Donaldson, D., T. Kahan, N. Kwamena, S. Handley, and C. Barbier (2009), Atmospheric chemistry of urban surface films, in *Atmospheric Aerosols Characterization, Chemistry, Modeling, and Climate*, edited, pp. 79-89, ACS Publications.
Falbe-Hansen, H., S. Sørensen, N. Jensen, T. Pedersen, and J. Hjorth (2000), Atmospheric gas-phase reactions of dimethylsulphoxide and dimethylsulphone with OH and NO3 radicals, Cl atoms and ozone, *Atmos. Environ.*, *34*(10), 1543-1551.
Fasnacht, M. P., and N. V. Blough (2003), Kinetic analysis of the photodegradation of polycyclic aromatic hydrocarbons in aqueous solution, *Aquat. Sci.*, *65*(4), 352-358.
Fasnacht, M. P., N. V. J. E. s. Blough, and technology (2002), Aqueous photodegradation of polycyclic aromatic hydrocarbons, *Environ. Sci. Technol.*, *36*(20), 4364-4369.
Frisch, M., G. Trucks, H. Schlegel, G. Scuseria, M. Robb, J. Cheeseman, G. Scalmani, V. Barone, G. Petersson, and H. Nakatsuji (2016), Gaussian 16, revision C. 01, edited, Gaussian, Inc., Wallingford CT.
Gaston, C. J., K. A. Pratt, X. Qin, and K. A. Prather (2010), Real-time detection and mixing state of methanesulfonate in single particles at an inland urban location during a phytoplankton bloom, *Environ. Sci. Technol.*, *44*(5), 1566-1572.
Glasow, R. v., and P. Crutzen (2004), Model study of multiphase DMS oxidation with a focus on halogens, *Atmospheric Chem. Phys.*, *4*(3), 589-608.
González-García, N., À. González-Lafont, and J. M. Lluch (2006), Variational transition-state theory study of the dimethyl sulfoxide (DMSO) and OH reaction, *J. Phys. Chem.A*, *110*(2), 798-808.
González-Gaya, B., M.-C. Fernández-Pinos, L. Morales, L. Méjanelle, E. Abad, B. Piña, C. M. Duarte, B. Jiménez, and J. Dachs (2016), High atmosphere–ocean exchange of semivolatile aromatic hydrocarbons, *Nat. Geosci*, *9*(6), 438-442, doi:10.1038/ngeo2714.
González-Gaya, B., A. Martínez-Varela, M. Vila-Costa, P. Casal, E. Cerro-Gálvez, N. Berrojalbiz, D. Lundin, M. Vidal, C. Mompeán, and A. Bode (2019), Biodegradation as an important sink of aromatic hydrocarbons in the oceans, *Nat. Geosci*, *12*(2), 119-125.
Grossman, J. N., A. P. Stern, M. L. Kirich, and T. F. Kahan (2016), Anthracene and pyrene photolysis kinetics in aqueous, organic, and mixed aqueous-organic phases, *Atmos. Environ.*, *128*, 158-164.
Guitart, C., N. Garcia-Flor, J. M. Bayona, and J. Albaiges (2007), Occurrence and fate of polycyclic aromatic hydrocarbons in the coastal surface microlayer, *Mar. Pollut. Bull.*, *54*(2), 186-194, doi:10.1016/j.marpolbul.2006.10.008.
Hanley, L., and R. Zimmermann (2009), Light and molecular ions: the emergence of vacuum UV single-photon ionization in MS, *Anal. Chem.*, *81*(11), 4174–4182.
Hardy, J. T., E. A. Crecelius, L. D. Antrim, S. L. Kiesser, V. L. Broadhurst, P. D. Boehm, W. G. Steinhauer, and T. H. Coogan (1990), Aquatic surface microlayer contamination in chesapeake bay, *Mar. Chem.*, *28*(4), 333-351.
Harvey, G. R., and R. F. Lang (1986), Dimethylsulfoxide and dimethylsulfone in the marine atmosphere, *Geophys. Res. Lett.*, *13*(1), 49-51.
Hatton, A., G. Malin, S. Turner, and P. Liss (1996), DMSO, A Significant Compound in the Biogeochemical Cycle of DMS., in *Biological and Environmental Chemistry of DMSP and Related Sulfonium Compounds*, edited, pp. 405-412, Springer.
Hoffmann, E. H., A. Tilgner, R. Schrodner, P. Brauer, R. Wolke, and H. Herrmann (2016), An advanced modeling study on the impacts and atmospheric implications of multiphase dimethyl sulfide chemistry, *Proc Natl Acad Sci U S A*, *113*(42), 11776-11781, doi:10.1073/pnas.1606320113.
Hopkins, R. J., Y. Desyaterik, A. V. Tivanski, R. A. Zaveri, C. M. Berkowitz, T. Tyliszczak, M. K. Gilles, and A. Laskin (2008), Chemical speciation of sulfur in marine cloud droplets and particles: Analysis of

individual particles from the marine boundary layer over the California current, *J. Geophys. Res-Atmos*, *113*(D4).
Hua, L., Q. Wu, K. Hou, H. Cui, P. Chen, W. Wang, J. Li, and H. Li (2011), Single photon ionization and chemical ionization combined ion source based on a vacuum ultraviolet lamp for orthogonal acceleration time-of-flight mass spectrometry, *Anal. Chem.*, *83*(13), 5309-5316.
Karl, M., A. Gross, C. Leck, and L. Pirjola (2007), Intercomparison of dimethylsulfide oxidation mechanisms for the marine boundary layer: Gaseous and particulate sulfur constituents, *J. Geophys. Res-Atmos*, *112*(D15), doi:10.1029/2006jd007914.
Kuang, B. Y., P. Lin, M. Hu, and J. Z. Yu (2016), Aerosol size distribution characteristics of organosulfates in the Pearl River Delta region, China, *Atmos. Environ.*, *130*, 23-35, doi:10.1016/j.atmosenv.2015.09.024.
Kukui, A., D. Borissenko, G. Laverdet, and G. Le Bras (2003), Gas-phase reactions of OH radicals with dimethyl sulfoxide and methane sulfinic acid using turbulent flow reactor and chemical ionization mass spectrometry, *J. Phys. Chem.A*, *107*(30), 5732-5742.
Lammel, G. (2015), Polycyclic aromatic compounds in the atmosphere–a review identifying research needs, *Polycyclic Aromat. Compd.*, *35*(2-4), 316-329.
Lee, P., and S. De Mora (1996), DMSP, DMS and DMSO concentrations and temporal trends in marine surface waters at Leigh, New Zealand, in *Biological and Environmental Chemistry of DMSP and Related Sulfonium Compounds*, edited, pp. 391-404, Springer.
Lee, P. A., S. J. de Mora, and M. Levasseur (1999), A review of dimethylsulfoxide in aquatic environments, *Atmosphere-Ocean*, *37*(4), 439-456, doi:10.1080/07055900.1999.9649635.
Legrand, M., J. Sciare, B. Jourdain, and C. Genthon (2001), Subdaily variations of atmospheric dimethylsulfide, dimethylsulfoxide, methanesulfonate, and non‐sea‐salt sulfate aerosols in the atmospheric boundary layer at Dumont d'Urville (coastal Antarctica) during summer, *J. Geophys. Res-Atmos*, *106*(D13), 14409-14422.
Liang, Y., D. R. Gardner, C. D. Miller, D. Chen, A. J. Anderson, B. C. Weimer, R. C. J. A. Sims, and e. microbiology (2006), Study of biochemical pathways and enzymes involved in pyrene degradation by Mycobacterium sp. strain KMS, *Appl. Environ. Microbiol.*, *72*(12), 7821-7828.
Librando, V., G. Bracchitta, G. de Guidi, Z. Minniti, G. Perrini, and A. Catalfo (2014), Photodegradation of anthracene and benzo [a] anthracene in polar and apolar media: new pathways of photodegradation, *Polycyclic Aromat. Compd.*, *34*(3), 263-279.
Librando, V., G. Tringali, J. Hjorth, and S. Coluccia (2004), OH-initiated oxidation of DMS/DMSO: reaction products at high NOx levels, *Environ. Pollut.*, *127*(3), 403-410.
Lohmann, R., R. Gioia, K. C. Jones, L. Nizzetto, C. Temme, Z. Xie, D. Schulz-Bull, I. Hand, E. Morgan, and L. J. E. s. Jantunen (2009), Organochlorine pesticides and PAHs in the surface water and atmosphere of the North Atlantic and Arctic Ocean, *Environ. Sci. Technol.*, *43*(15), 5633-5639.
Ma, Y., Z. Xie, H. Yang, A. Möller, C. Halsall, M. Cai, R. Sturm, and R. Ebinghaus (2013), Deposition of polycyclic aromatic hydrocarbons in the North Pacific and the Arctic, *J. Geophys. Res-Atmos*, *118*(11), 5822-5829.
Mandal, D., S. Bagchi, and A. K. Das (2012), Mechanism and kinetics for the reaction of O (3P) with DMSO: A theoretical study, *Chem. Phys. Lett.*, *551*, 31-37.
McLean, A., and G. Chandler (1980), Contracted Gaussian basis sets for molecular calculations. I. Second row atoms, Z= 11–18, *J. Chem. Phys.*, *72*(10), 5639-5648.
Mekic, M., J. Zeng, B. Jiang, X. Li, Y. G. Lazarou, M. Brigante, H. Herrmann, and S. Gligorovski (2020a), Formation of Toxic Unsaturated Multifunctional and Organosulfur Compounds From the Photosensitized Processing of Fluorene and DMSO at the Air‐Water Interface, *J. Geophys. Res-Atmos*, *125*(6), doi:10.1029/2019jd031839.
Mekic, M., J. Zeng, W. Zhou, G. Loisel, B. Jin, X. Li, D. Vione, and S. Gligorovski (2020b), Ionic Strength Effect on Photochemistry of Fluorene and Dimethylsulfoxide at the Air–Sea Interface: Alternative Formation Pathway of Organic Sulfur Compounds in a Marine Atmosphere *ACS Earth Space Chem.*, *4*(7), 1029-1038, doi:10.1021/acsearthspacechem.0c00059.

Monge, M. E., C. George, B. D'Anna, J.-F. Doussin, A. Jammoul, J. Wang, G. Eyglunent, G. Solignac, V. Daele, and A. Mellouki (2010), Ozone formation from illuminated titanium dioxide surfaces, *J. Am. Chem. Soc.*, *132*(24), 8234-8235.
Mopper, K. K., David J. (2002), Photochemistry and the cycling of carbon, sulfer, nitrogen and phosphorus, in *Biogeochemistry of marine dissolved organic matter*, edited, pp. 455-508, Elsevier Science, USA.
Nelson, N. B., and D. A. Siegel (2013), The global distribution and dynamics of chromophoric dissolved organic matter, *Annu. Rev. Mar. Sci.*, *5*, 447-476.
Ning, A., H. Zhang, X. Zhang, Z. Li, Y. Zhang, Y. Xu, and M. Ge (2020), A molecular-scale study on the role of methanesulfinic acid in marine new particle formation, *Atmos. Environ.*, *227*, doi:10.1016/j.atmosenv.2020.117378.
Nizkorodov, S. A., J. Laskin, and A. Laskin (2011), Molecular chemistry of organic aerosols through the application of high resolution mass spectrometry, *PCCP*, *13*(9), 3612-3629.
O'Dowd, C. D., M. C. Facchini, F. Cavalli, D. Ceburnis, M. Mircea, S. Decesari, S. Fuzzi, Y. J. Yoon, and J.-P. Putaud (2004), Biogenically driven organic contribution to marine aerosol, *Nature*, *431*(7009), 676-680.
Otto, S., T. Streibel, S. Erdmann, S. Klingbeil, D. Schulz-Bull, and R. Zimmermann (2015), Pyrolysis–gas chromatography–mass spectrometry with electron-ionization or resonance-enhanced-multi-photon-ionization for characterization of polycyclic aromatic hydrocarbons in the Baltic Sea, *Mar. Pollut. Bull.*, *99*(1-2), 35-42.
Pérez-Carrera, E., V. M. L. León, A. G. Parra, and E. González-Mazo (2007), Simultaneous determination of pesticides, polycyclic aromatic hydrocarbons and polychlorinated biphenyls in seawater and interstitial marine water samples, using stir bar sorptive extraction–thermal desorption–gas chromatography–mass spectrometry, *J. Chromatogr. A*, *1170*(1-2), 82-90.
Pope, F., J. Nicovich, and P. Wine (2002), A temperature‐dependent kinetics study of the reaction of O (3PJ) with (CH3) 2SO, *Int. J. Chem. Kinet.*, *34*(3), 156-161.
Rehmann, K., N. Hertkorn, and A. A. Kettrup (2001), Fluoranthene metabolism in Mycobacterium sp. strain KR20: identity of pathway intermediates during degradation and growth, *Microbiology*, *147*(10), 2783-2794.
Richards, S., J. Rudd, and C. Kelly (1994), Organic volatile sulfur in lakes ranging in sulfate and dissolved salt concentration over five orders of magnitude, *Limnol. Oceanogr.*, *39*(3), 562-572.
Ridgeway, R. G., D. C. Thornton, and A. R. Bandy (1992), Determination of trace aqueous dimethylsulfoxide concentrations by isotope dilution gas chromatography/mass spectrometry: Application to rain and sea water, *J. Atmos. Chem.*, *14*(1-4), 53-60.
Riffault, V., Y. Bedjanian, and G. Le Bras (2003), Kinetics and mechanism of the O atom reaction with dimethyl sulfoxide, *J. Phys. Chem.A*, *107*(28), 5404-5411.
Schobesberger, S., et al. (2013), Molecular understanding of atmospheric particle formation from sulfuric acid and large oxidized organic molecules, *Proc Natl Acad Sci U S A*, *110*(43), 17223-17228, doi:10.1073/pnas.1306973110.
Seidel, M., M. Manecki, D. P. Herlemann, B. Deutsch, D. Schulz-Bull, K. Jürgens, and T. Dittmar (2017), Composition and transformation of dissolved organic matter in the Baltic Sea, *Front. Earth Sci.*, *5*, 31.
Stortini, A., T. Martellini, M. Del Bubba, L. Lepri, G. Capodaglio, and A. Cincinelli (2009), n-Alkanes, PAHs and surfactants in the sea surface microlayer and sea water samples of the Gerlache Inlet sea (Antarctica), *Microchem. J.*, *92*(1), 37-43.
Styler, S., M.-E. Loiseaux, and D. Donaldson (2011), Substrate effects in the photoenhanced ozonation of pyrene, *Atmospheric Chem. Phys.*, *11*(3), 1243-1253.
Tao, S., X. Lu, N. Levac, A. P. Bateman, T. B. Nguyen, D. L. Bones, S. A. Nizkorodov, J. Laskin, A. Laskin, and X. Yang (2014a), Molecular characterization of organosulfates in organic aerosols from Shanghai and Los Angeles urban areas by nanospray-desorption electrospray ionization high-resolution mass spectrometry, *Environ. Sci. Technol.*, *48*(18), 10993-11001, doi:10.1021/es5024674.
Tao, S., X. Lu, N. Levac, A. P. Bateman, T. B. Nguyen, D. L. Bones, S. A. Nizkorodov, J. Laskin, A. Laskin, and X. Yang (2014b), Molecular characterization of organosulfates in organic aerosols from Shanghai

and Los Angeles urban areas by nanospray-desorption electrospray ionization high-resolution mass spectrometry, *Environ. Sci. Technol.*, *48*(18), 10993-11001.
Urbanski, S., R. Stickel, and P. Wine (1998), Mechanistic and kinetic study of the gas-phase reaction of hydroxyl radical with dimethyl sulfoxide, *J. Phys. Chem.A*, *102*(51), 10522-10529.
Vácha, R., P. Jungwirth, J. Chen, and K. Valsaraj (2006), Adsorption of polycyclic aromatic hydrocarbons at the air–water interface: Molecular dynamics simulations and experimental atmospheric observations, *PCCP*, *8*(38), 4461-4467.
Valavanidis, A., T. Vlachogianni, S. Triantafillaki, M. Dassenakis, F. Androutsos, and M. Scoullos (2008), Polycyclic aromatic hydrocarbons in surface seawater and in indigenous mussels (Mytilus galloprovincialis) from coastal areas of the Saronikos Gulf (Greece), *Estuar. Coast. Shelf Sci.*, *79*(4), 733-739.
van Herwijnen, R., P. Wattiau, L. Bastiaens, L. Daal, L. Jonker, D. Springael, H. A. Govers, and J. R. Parsons (2003), Elucidation of the metabolic pathway of fluorene and cometabolic pathways of phenanthrene, fluoranthene, anthracene and dibenzothiophene by Sphingomonas sp. LB126, *Res. Microbiol.*, *154*(3), 199-206.
Vasilkov, A., N. Krotkov, J. Herman, C. McClain, K. Arrigo, and W. Robinson (2001), Global mapping of underwater UV irradiances and DNA‐weighted exposures using Total Ozone Mapping Spectrometer and Sea‐viewing Wide Field‐of‐view Sensor data products, *J. Geophys. Res. Oceans*, *106*(C11), 27205-27219.
Wang, X. K., S. Rossignol, Y. Ma, L. Yao, M. Y. Wang, J. M. Chen, C. George, and L. Wang (2016), Molecular characterization of atmospheric particulate organosulfates in three megacities at the middle and lower reaches of the Yangtze River, *Atmospheric Chem. Phys.*, *16*(4), 2285-2298, doi:10.5194/acp-16-2285-2016.
Weigend, F. (2006), Accurate Coulomb-fitting basis sets for H to Rn, *PCCP*, *8*(9), 1057-1065.
Weigend, F., and R. Ahlrichs (2005), Balanced basis sets of split valence, triple zeta valence and quadruple zeta valence quality for H to Rn: Design and assessment of accuracy, *PCCP*, *7*(18), 3297-3305.
Wilkinson, F., W. P. Helman, and A. B. Ross (1995), Rate constants for the decay and reactions of the lowest electronically excited singlet state of molecular oxygen in solution. An expanded and revised compilation, *J. Phys. Chem. Ref. Data*, *24*(2), 663-677.
Wurl, O., E. Wurl, L. Miller, K. Johnson, and S. Vagle (2011), Formation and global distribution of sea-surface microlayers, *Biogeosciences*, *8*(1), 121-135, doi:10.5194/bg-8-121-2011.
Zhang, L., I. Kuniyoshi, M. Hirai, and M. Shoda (1991), Oxidation of dimethyl sulfide byPseudomonas acidovorans DMR-11 isolated from peat biofilter, *Biotechnol. Lett*, *13*(3), 223-228.
Zhang, M., W. Gao, J. Yan, Y. Wu, C. A. Marandino, K. Park, L. Chen, Q. Lin, G. Tan, and M. Pan (2019), An integrated sampler for shipboard underway measurement of dimethyl sulfide in surface seawater and air, *Atmos. Environ.*, *209*, 86-91.
Zhang, S. H., G. P. Yang, H. H. Zhang, and J. Yang (2014), Spatial variation of biogenic sulfur in the south Yellow Sea and the East China Sea during summer and its contribution to atmospheric sulfate aerosol, *Sci. Total Environ.*, *488-489*, 157-167, doi:10.1016/j.scitotenv.2014.04.074.
Zhao, H., X. Jiang, and L. Du (2017), Contribution of methane sulfonic acid to new particle formation in the atmosphere, *Chemosphere*, *174*, 689-699, doi:10.1016/j.chemosphere.2017.02.040.
Zhao, Y., and D. G. Truhlar (2008), The M06 suite of density functionals for main group thermochemistry, thermochemical kinetics, noncovalent interactions, excited states, and transition elements: two new functionals and systematic testing of four M06-class functionals and 12 other functionals, *Theor. Chem. Acc.*, *120*(1), 215-241.
Zhou, S., B. C. H. Hwang, P. S. J. Lakey, A. Zuend, J. P. D. Abbatt, and M. Shiraiwa (2019), Multiphase reactivity of polycyclic aromatic hydrocarbons is driven by phase separation and diffusion limitations, *Proc. Natl. Acad. Sci. U. S. A.*, *116*(24), 11658-11663, doi:10.1073/pnas.1902517116.
Zhu, M., et al. (2019), Organosulfur Compounds Formed from Heterogeneous Reaction between SO2 and Particulate-Bound Unsaturated Fatty Acids in Ambient Air, *Environ. Sci. Technol. Lett.*, *6*(6), 318-322, doi:10.1021/acs.estlett.9b00218.